10.1515/tvsb-2015-0014

**Transactions of the VŠB – Technical University of Ostrava**

Civil Engineering Series, No. 2, Vol. 15, 2015

paper #14

**Nguyen Nam Hai LUU** [1]

# ANALYTICAL SIMPLIFY MODELS OF THE KEY ELEMENTS IN THE ALTERNATIVE LOAD PATH WITHIN THE FRAME IN ACCIDENTAL SITUATION

**Abstract**

The present document is dedicated to global behavior of a frame further to the loss of a column, taking into account the redistribution of the internal forces. Structural elements, transfer the load to the foundation, are isolated as key elements. Two possible alternative load paths in the investigated event are described. The proposal on the local investigation of the important sub structure instead of full global frame's assessment reveal the internal forces distribution along the alternative load path is demonstrated.

**Keywords**

Progressive collapse, multi-storey building, loading sequence, alternative load path, key elements, catenary action.

## 1 INTRODUCTION

### 1.1 Alternative load path

Officially provided worldwide in codes and many other provisions, the direct design method using the "alternative load path" approach is usually addressed in official documents on progressive collapse prevention. From a different standpoint, the alternative load path method can be described as the search for a structure's defense against the propagation of failure. According to Ettouney (2004) and Smilowitz (2007), the initial damage propagates through the building structure and forms a "failure front". The failure front spreads outwards from the initial damaged region. Therefore, at a given instant during the propagation process, only a small portion of the structure needs to be investigated because the outer structural properties do not affect the current damaged region. And because the column's axial stiffness is typically greater than the beam's bending stiffness, the vertical propagation of the failure front is faster than the horizontal one. In normal structural geometry, the horizontal failure front goes through the beam-to-column points and causes flexural yield in the beam end-section but not across the column line. In the region adjoining the damaged one, the beam may form a flexural hinge, fail in shear or undergo axial failure due to a catenary action.

In many articles, alternative load path assessment has been discussed. Examples of these articles are case studies such as Powell (2004), proposals for an alternative load path analysis method as in Elvira et al. (2005) or designs to prevent progressive collapse by increasing frame redundancy, proved by an efficient alternative load path and taking into account the flexural and axial deformations, as in Hamburger and Whittaker (2002). However, they only described general guidelines for solving the problem of the assessment of a structure's capacity.

[1] PhD. Luu Nguyen Nam Hai, Engineering Foundation department, Civil Engineering fakulty, Ton Duc Thang university, 19- Nguyen Huu Tho, Tan Phong ward, district 7, Ho Chi Minh city, Vietnam, luunguyennamhai@tdt.edu.vn.

Recently, the intriguing method described in J. Agarwal et al. (2003) and in England, Agarwal, and Blockley (2008) provides a mathematical solution to the automatic estimation of the alternative load path within the existing building frame. Agarwal's work presents a method for enumerating the structure members and creates a hierarchical description of the frame configuration. Through structural hierarchy, different vulnerability scenarios are predicted. In this way, the alternative load paths and the key elements are pointed out based on the connectivity of the structural elements.

Agarwal's method has the advantage of automatically predicting the "failure front" within any arbitrary structure. It is general and already developed in 2D and 3D. However, as shown in the figure above, even a simple structure will be described by a complex hierarchy. This is because the process requires complex calculations and is solved by PC programming. With the exception of this article, even though the alternative load path method has been widely proposed on provisions and in other articles, no diaphragm solution had been provided until this time.

## 1.2 Catenary action

As discussed before, the membrane effect or catenary action is accepted as the solution to the increase in frame redundancy in an abnormal situation. However, as in the case of the alternative load path method, this solution appeared many times in general guidelines and in experts' reports but there was a lack of information on processing and analytical solutions.

According to Hamburger and Whitaker (2002), in a catastrophic situation, a steel frame should be designed in order to have the capacity to withstand the large tensile demand simultaneously applied with large inelastic flexural deformations. However, the article is limited to design strategies and the idea of design applications. No analytical model or detailed prediction of catenary phenomena is presented.

In the same proceedings of the National Workshop on Prevention of Progressive Collapse, held on July 10-12, 2002, Ahmad Rahimian and Kamran Moazami (2002) proposed a method to increase frame integrity by expanding the alternative load path with the catenary action. The case study of a 35-story composite building, with full-scale numerical simulations, was carried out to investigate the structural behavior and to provide integrity criteria. A restrained spring was placed at the beam end and it is defined as K. According to the authors, the value K comes from the adjacent columns close to the damaged one.

Yin and Wang (2005) developed the analytical model of the catenary action in steel beams under different temperature conditions. They provide the nonlinear model with the two inelastic and plastic interactions between the axial force and bending moment in the catenary beams are covered. Demonceau (2007) predicted the behavior of the beams directly above the damaged column when plastic hinges appeared. A simplified substructure model was extracted from the frame with some parameters had to be predicted. The simplified analytical models developed in [Demonceau,2008] to predict the latter are presented in the following sections.

Parallel to Demonceau's research, an investigation and development of the same aspect were performed at Imperial University in the UK by Izzuddin and Vlassis (2007). In order to develop the multi-level assessment of a 3D building's robustness due to the sudden loss of a column, the 3-step reduction procedure is applied to explain the neighboring column's capacity to withstand the load redistribution. The columns in the same line with the damaged one are not taken into account. In [Izzuddin and al, 2007] and Vlassis's thesis, the models which are presented to compute this curve are based on rough assumptions, in particular for the computation of the parameters to be used within the models.

### 1.3 The content of this article

This paper, focus on the separation of the local zones on the alternative load path, in order to investigate the global behaviour of the building's frame. Based on the illustration of how to physical translate the load application on building process to the evolution of the damage column's axial forces, the nature of an exceptional event "column lost" is described in section 2 and 3. Section 2 presents the methodologies followed during the investigations conducted throughout the research. In particular, the building frames are separated according to different zones, representing parts of the frame which are influenced by the column loss.

Section 2 also discusses the development of the alternative load paths within the damaged structure after the event of the loss of a column. In particular, numerical simulations of the frame under the load sequence described in section 3 are carried out on the building frames. Based on these results, structural elements, which transfer the load to the foundation, are isolated. These elements form the alternative load paths. Two possible load paths in the event investigated are described.

Next, section 4 concentrates on a part of the frame which is directly affected by the loss of column event. This paragraph describes the distribution of the internal forces within the part above the damaged column. This structural part is extracted from the frame. An analytical model of the part, representing its behaviour, is developed and validated.

Section 5 analyzes behavior of the column in the alternative load path. Two columns, which are placed on both sides of the damaged column, support an extreme load. This chapter describes the development of an analytical model to predict the compression on these columns. Based on this model, a critical element, which undergoes a high combination of compression and bending, is extracted as a key element.

## 2 COLUMN LOSS SIMULATION AND ASSUMPTIONS

The loss of the column can be associated to different types of exceptional actions: explosion, impact of a vehicle,… which is not directly considered in the design process. Under some of these exceptional actions, dynamic effects may play an important role; within the present work, it is assumed that the action associated to the column loss does not induce significant dynamic effects. So, the performed investigations are based on static approaches.

Accordingly, the column is assumed to be progressively removed from the frame and the normal load within this column varies progressively from the one appearing under the "normal" design loads to 0 (when the column is completely removed from the frame). This simulation, trying to repeat the true action of real frame, translates the physical manner to the progressively exceptional removal of column.

Fig. 2. a represents a frame where the damaged column is column **AB**. Uniformly distributed loads are applied to each beam and column (to simulate design loads such as self-weight, permanent loads, and live loads). For simplicity's sake, the wind loads are not represented.

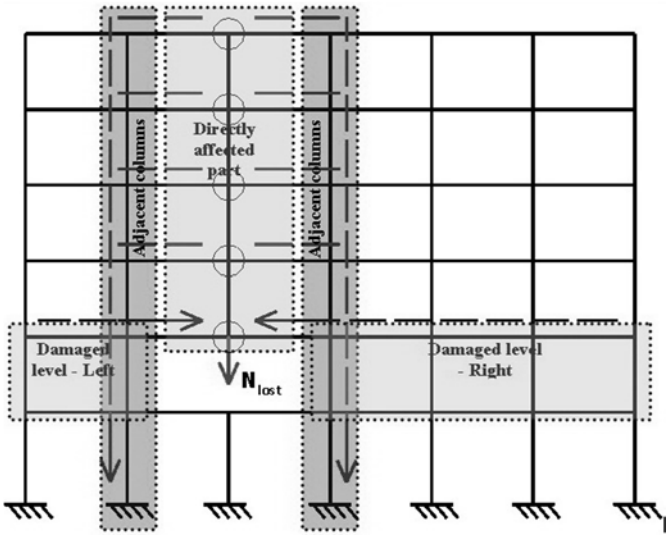


Fig. 1: Representation of a frame losing a column

In Fig. 2, the curve representing the evolution of the normal load in column AB (NAB) according to the vertical displacement at point A is illustrated:

- At point (1), the frame is not loaded; hence, $N_{AB}$ and $\Delta_A$ are equal to 0.
- From point (1) to (2) (Phase 1), the design loads are progressively applied, i.e normal loading is applied to the structure; hence, $N_{AB}$ progressively decreases (as column **AB** is subjected to compression) while $\Delta_A$ can be assumed to be equal to 0 during this phase. (In reality, there is a small vertical displacement at point A attributable to the compression of the columns below point **A**.) It is assumed that no yielding appears in the investigated frame during this phase, i.e., the frame remains fully elastic.
- From point (2) to (5), the column progressively disappears. Indeed, from point (2) on, the compression $N_{AB}$ in column **AB** decreases until it reaches a value equal to 0 (i.e., no more axial loads in the lost column) at point (5) which means that the column can be considered fully destroyed. So, in this zone, the value of $N_{AB}$ progressively decreases while the value of $\Delta_A$ increases. This part of the graph is divided into two phases as represented in Fig. 2:
    - From point (2) to (4) (Phase 2): during this phase, the directly affected part passes from fully elastic behavior (from point (2) to (3)) to a plastic mechanism (beam mechanism on each floor of the directly affected part) (at point (4)). At point (3), the first plastic hinges appear in the directly affected part.
    - From point (4) to (5) (Phase 3): during this phase, high deformations of the directly affected part are observed and second order effects play an important role. In particular, significant catenary actions develop in the bottom beams of the directly affected part. It is only possible to pass from point (1) to (5) if:
- the loads which are transferred from the directly affected part to the indirectly affected part do not induce the collapse of elements in the latter (for instance, buckling of the columns or formation of a global plastic mechanism in the indirectly affected part);
- the compression loads appearing in the upper beams of the directly affected part (corresponding to an “arch” effect) do not lead to the buckling of the latter;
- the different structural elements have a sufficient level of ductility to reach the vertical displacement corresponding to point (5).

Also, it is possible that the complete removal of the column is reached (i.e., $N_{AB} = 0$) before reaching Phase 3. The exceptional event is illustrated in Fig. 2, representing the evolution of the axial load within the lost column according to the vertical displacement at the top of this column.

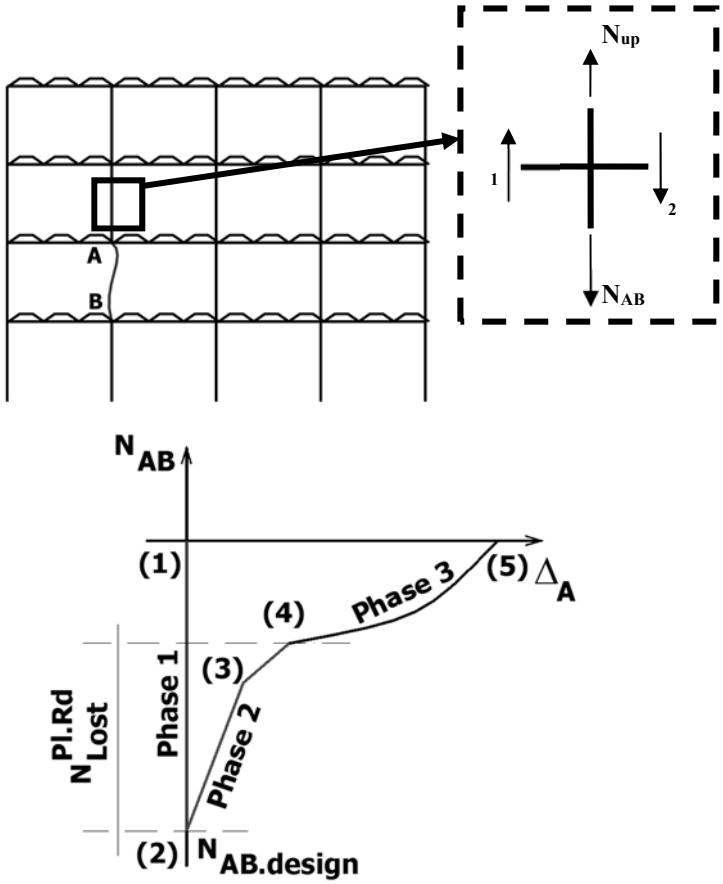


Fig. 2: Column axial force and Y displacement of the top of a collapsed column

## 3 ADDITIONAL LOADS RELATED TO THE LOSS OF A COLUMN

In the frame's *initial state*, the loads to be supported are the conventional ones as defined in the codes and standards. After the column loss due to an exceptional event, the remaining structure is in its *residual state*. To pass from the initial to the *residual state*, the applied loads are assumed to constant, i.e. only the structural system is modified. As illustrated in Fig. 3, two loading sequences have been defined to pass from the *initial* to the *residual state*.

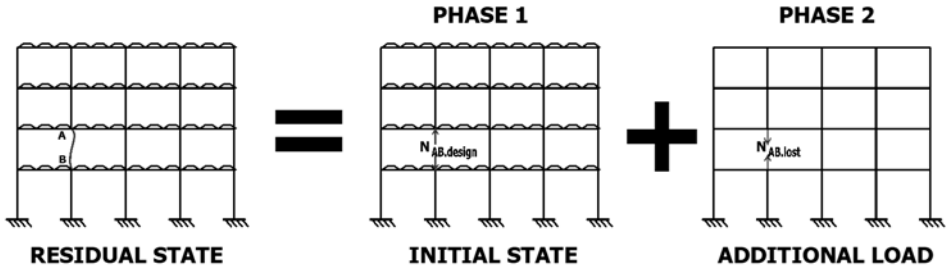


Fig. 3: Identification of two loading sequences

With the assumption of a progressive removal of the column, the axial load in the lost column is progressively reduced from the design value, i.e. its value in the initial state, to zero. These loads are concentrated forces applied at the top and at the bottom of the lost column in the direction opposite to the column's internal forces in the initial state, named $N_{AB,design}$. The value of the loads associated with the column loss, named $N_{AB.lost}$, is as follows:

$$0 \leq N_{AB.lost} \leq N_{AB.design} \tag{1}$$

## 4 INTERNAL FORCE DISTRIBUTION IN THE DIRECTLY AFFECTED PART

### 4.1 Distribution of internal forces

As presented, the load sequence applied to the frame is demonstrated by a load-carrying curve.

**Phase one**: From point (1) to point (2), the design load is applied to the frame. It is in its *initial state*. The frame is illustrated with one modification to its physical configuration: the damaged column is replaced by its normal force. At point (1), the frame is not loaded. From point (1) to (2), the design loads are applied progressively. A compression force appears in the middle columns and progressively increases due to the applied load. Then, a bending moment and shear force appear in the equivalent beams as demonstrated in Fig. 4.

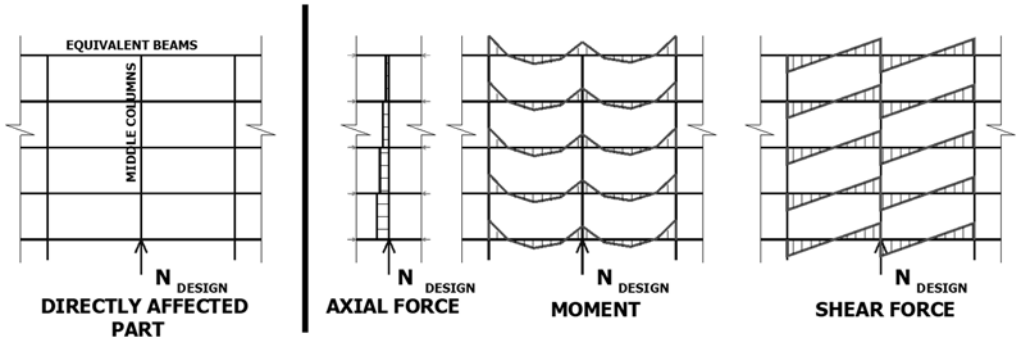


Fig. 4: Distribution of the internal forces in the initial state

**Phase 2**: From point (2) to point (4), the column progressively disappears. The frame goes from its *initial state* to a *residual state*. The axial force $N_{AB}$ of the damaged column progressively increases. Fig. 6.3.b illustrates the **Load Phase 2** from point (2) to point (4). Point (3) corresponds to the first plastic hinge's appearance in the directly affected part. While the frame goes from point (2) to point (3), its behavior is fully elastic. As soon as the first plastic hinge is formed within the directly affected part, the frame's behavior is no longer elastic.

Accordingly, the evolution of the loads when passing from the *initial* to the *residual state* is linked to the evolution of the loads due to the column loss. These loads are concentrated forces applied at the top and bottom of the lost column in the direction opposite to the column's internal forces in its initial state, called $N_{design}$. The value of the loads due to the column loss is named $N_{lost}$. Thus, the internal forces' form and magnitude within the directly affected part change, as seen in Fig. 5. Here, the bending moments in the section next to the middle columns increase while the values at both ends of the section closest to the adjacent columns decrease. Likewise, the shear forces change according to the variation in the bending moment. Their evolution is described in the next paragraph to highlight the danger inherent in this part's position.

However, the disappearance of the damaged column produces a special phenomenon within the directly affected part. This part acts as an "arch", bridging over the damaged position. The arch effect describes the special behavior of the directly affected part and surrounding members resulting in the development of a fictitious arch over the damaged column. This is achieved by the distribution

of the beam's normal forces. The axial forces appearing within the equivalent beams are distributed as demonstrated in Fig. 5. The top beams are compressed, while the bottom beams are under tension.

The axial force within the middle columns is directly linked to the progressive disappearance of the damaged column. Its distribution does not change, but its magnitude decreases. This is also discussed in the next paragraph on **Phase 3**.

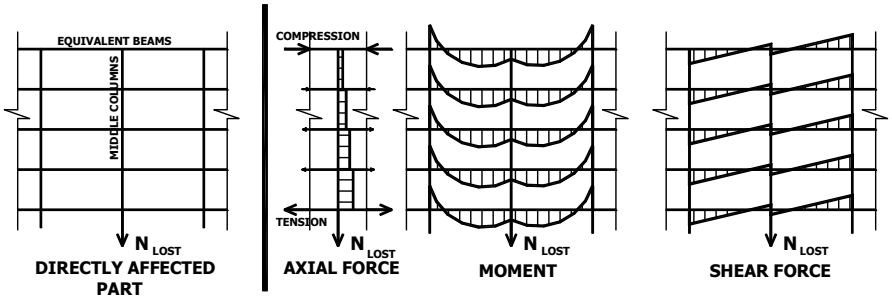


Fig. 5: Distribution of the internal forces in the residual state

**Phase 3**: In the case where the maximum value of $N_{design}$ is higher than the directly affected part's resistance $N_{lost}^{Pl.Rd}$, and where a catenary action could arise, the frame can go from point (4) to point (5) in Fig. 6.3. When point (4) is reached, the equivalent beam's end sections fully yield. Each equivalent beam then becomes a mechanism. In this case, the bending moment's values at the yield positions are equal to that section's plastic resistances. In other words, the bending moment diagram does not change in this segment. Depending on the bending moment's values, the shear force's distribution remains at point (4).

Without the suspension of the upper structures, the damaged column's top point falls rapidly. Thus, the second-order phenomenon is activated in the bottom beams of the directly affected part. Membrane forces develop in that beam, as demonstrated in Fig. 6. The middle columns are attached to the catenary beam and so follow its deflection. Its axial forces remain constant between points (4) and (5).

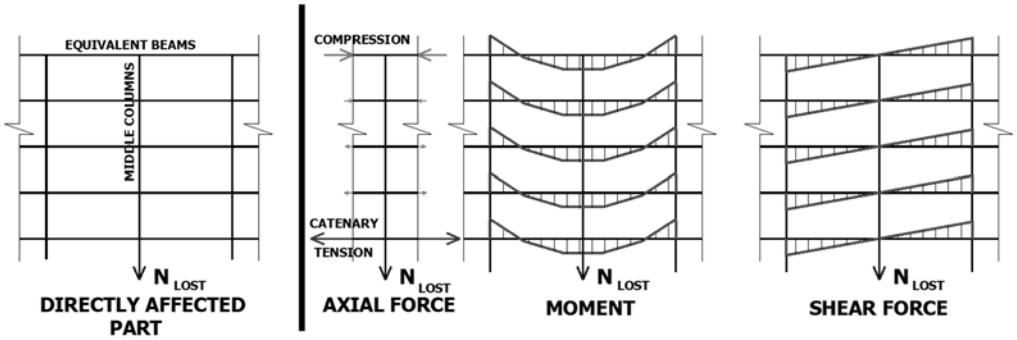


Fig. 6: Internal force distribution in Phase 3; catenary forces increase

The next section concentrates on the individual members' behavior in this zone of the frame.

## 4.2 Key members and sections

***The end sections of the equivalent beams***: In the investigation of the directly affected part, the equivalent beam appeared to be the most precarious member due to the sudden increase in its length and load. Indeed, the highest bending moment appears at that beam's end sections.

Fig. 7 presents the bottom beam, which connects points A, B, and C, more closely.

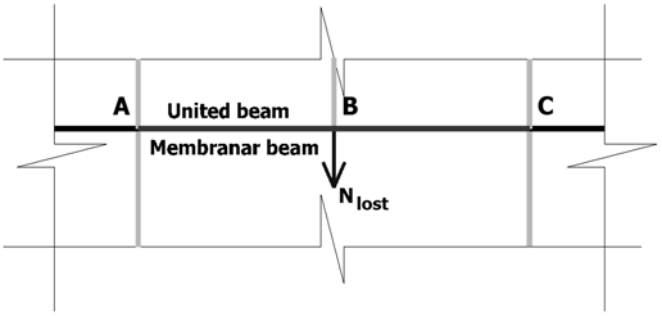


Fig. 7: Isolated membrane beam

Fig. 8.a demonstrates the bending moment diagram of the equivalent beam at point (2). At that moment, i.e., the initial state, the bending moment correlates to the initial state and so is called $M_{design}^{+,-}$. From point (2) to point (4), the additional load is gradually transferred to the beam as a result of the progressive disappearance of the column. This load produces additional internal forces within the frame. In the beam being studied, this load is called $M_{lost}^{+,-}$.

After that, Fig. 8.b presents the bending moment of the additional state. Before point (3), the frame's behavior is still within the elastic range. At this point, the bending moment's distribution is composed of both initial and additional states and behaves as seen below in Fig. 8.c.

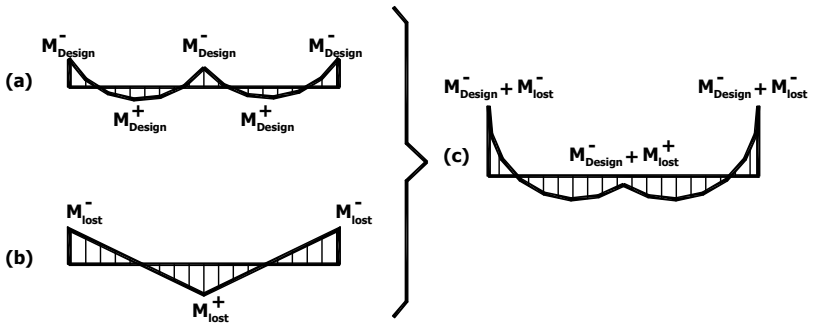


Fig. 8: Bending moment diagram of equivalent beam in Phase 2
(a) Initial state; (b) Additional state;
(c) Bending moment of the equivalent beam within the elastic range.

***The axial force in the beams***: After point (2), axial forces appear in the directly affected beams. Those beams are pulled or pushed according to the deformation of the adjacent columns on both sides. Compression appears in the top beam while tension acts on the bottom beam. Fig. 9 presents the distribution of these axial forces along the height of the directly affected part.

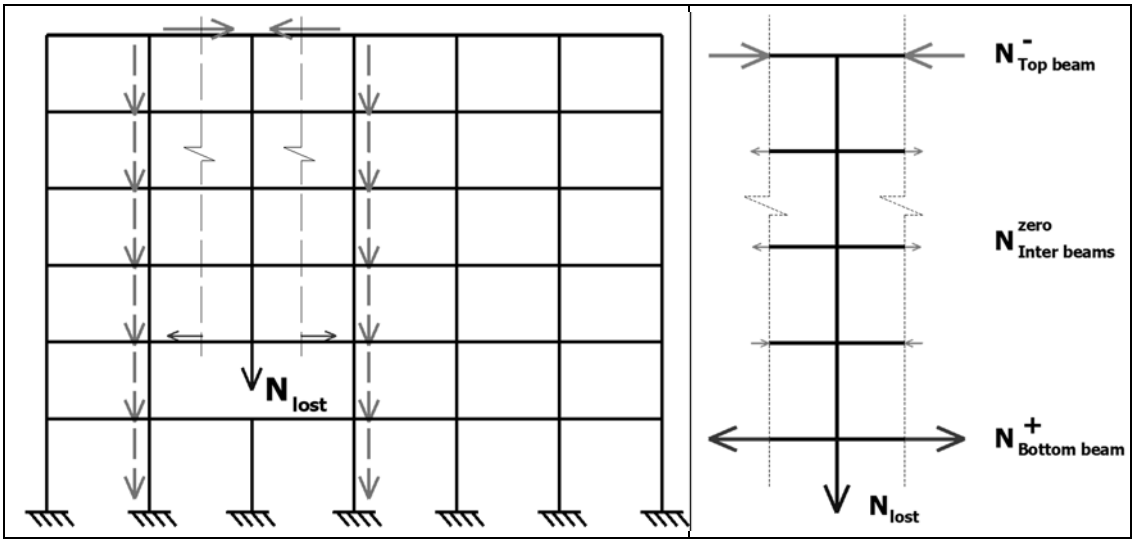


Fig. 9: Axial forces in the directly affected beams

Thus, even though the bending moments, which appear in the beams, are similar, the bottom and top beams support a different level of loading. This internal force distribution is described as an arch effect. As mentioned above, this type of behavior will be explained more later on.

Another consequence is the activation of the catenary effect in the directly affected part. In Fig. 2, point (4) corresponds to the total yielding of this part. The equivalent beam's end sections are at their limit state at that point. After point (4), the top and intermediate beams still keep their initial states, with the axial force being negative or nearly zero. Only the bottom beam, with its initial level of tension, could activate a catenary action.

## 5 DISTRIBUTION OF INTERNAL FORCES AND DISPLACEMENT OF SPECIFIC POINTS

This section describes the distribution of internal forces within the frame in its residual state. To illustrate the influence of the members adjacent to the column, the extended zone has been demonstrated in Fig. 10. Instead of concentrating only on the adjacent columns zone, the investigated zone was extended by one column on each side.

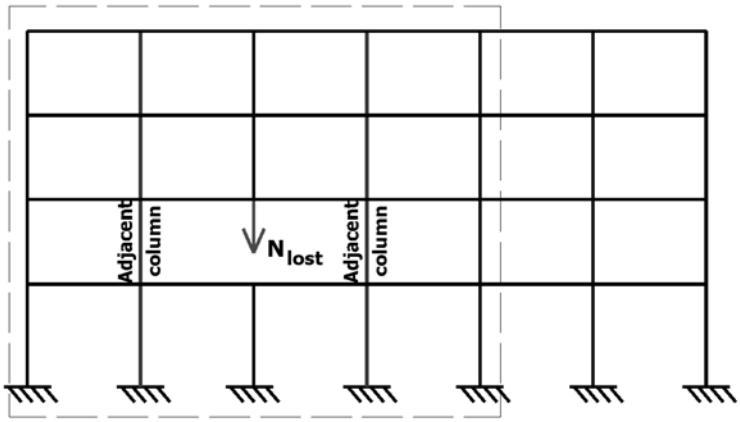


Fig. 10: The investigated zone in the residual frame

As presented before, the residual frame was then investigated in two separate loading states, i.e., the design and additional loading states.

## 5.1 Loading phases and the additional load

Fig. 11. illustrates the distribution of bending moment and axial forces in the residual frame in Load Phase 2. As discussed in previous section, the load was separated into two loading states. The first state in Load Phase 2 corresponds to the maximum state of Load Phase 1 at point (2). The second state is comprised of the additional load in which the residual frame supports the pair of concentrated forces representing the column's gradual disappearance. By analyzing how the residual frame supports this load, the nature of a frame's response following the loss of a column was revealed.

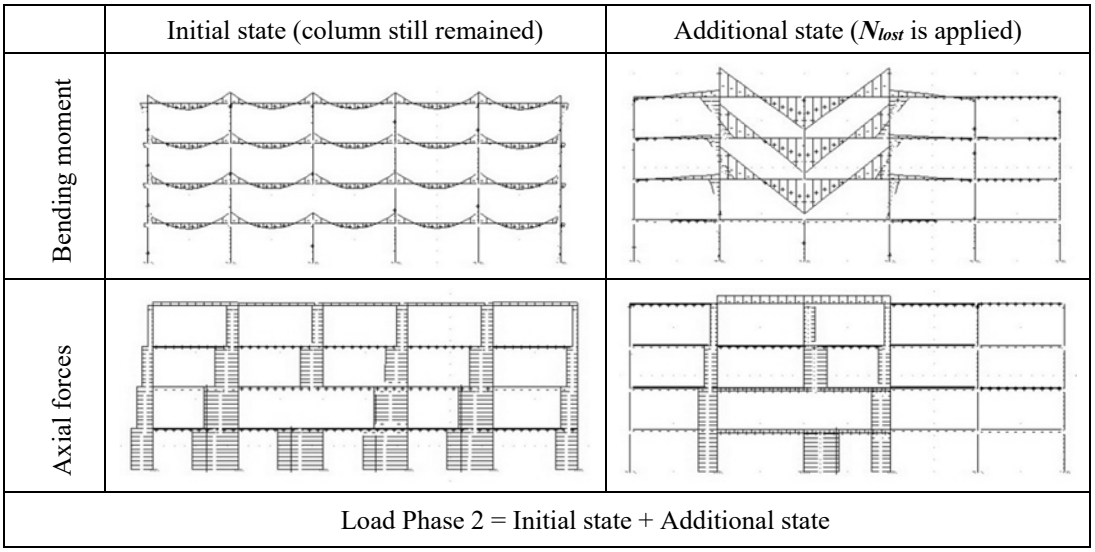


Fig. 11: The distribution of internal forces in the residual frame in Load Phase 2

## 5.2 The arch effect and the axial force in the beams

In section 4, the behavior of the directly affected part was investigated in order to calculate its critical resistance $N_{lost}^{Pl.Rd}$. The distribution of bending moment was illustrated to describe the development of the substructure visually, at which point the arrangement of axial forces in each beam was also briefly described.

The "arch effect," as it is called, is a phenomenon found in the residual frame, which must support the additional load, thereby forming an arch over the damaged position. The arch transfers the load to both sides of the damaged hole and produces horizontal compression on the members over the hole. The diagonal forces appearing in the wall above the lintel over a window is a comparative example of this arch phenomenon, as in Fig. 12.a.

In fact, when applying the additional load, above the directly affected part, axial forces appear in the equivalent beam due to the deformation of the adjacent columns.

The bending moment, which comes from the directly affected part, bends the adjacent columns. Depending on the capacity for horizontal movement on the left and right floors, the column deforms toward the center of the directly affected part. This deformation produces compression in the top equivalent beam and a smaller magnitude of tension in the bottom beam. According to the arrangement of the adjacent columns' and equivalent beam's stiffness, the axial forces within the

equivalent beams changed. In particular, in a typical frame, the intermediate equivalent beam's axial force magnitude was very close to zero.

In fact, this phenomenon occurs only in the case where the adjacent column's end points can move horizontally. Therefore, if the frame is braced on both sides and the beam lengthens only slightly, the arch effect disappears.

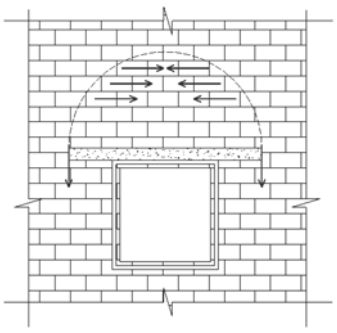

(a) Arch effect over the lintel

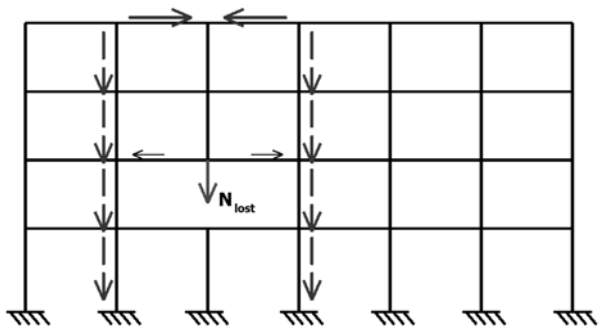


(b) Top and bottom beam axial force due to arch effect

Fig. 12: The distribution of axial forces in the equivalent beam due to the arch effect

### 5.4 Compression on the adjacent columns

Fig. 13 demonstrates the distribution of axial forces and bending moment in the adjacent columns' zone during the additional loading state. On each floor, the equivalent beam receives pressure from the middle column and bends. Then the bending moment and shear forces are transferred to the adjacent column. From the top floor to the membrane beam, the adjacent columns' axial force increases floor by floor. On the floor under the damaged column, the axial forces are transferred from the columns above. Their magnitude remains unchanged from that of the columns on the damaged floor.

So, on each floor, the adjacent columns section must support a combined load of compression and bending moment. It is very clear that the column next to the damaged one must withstand the highest pair of (***M, N***). Since Load Phase 2 consists of a combination of two loading states, the axial force and bending moment in the adjacent columns equals the sum of two values (in the elastic range):

$$\begin{aligned} N_{phase2} &= N_{design} + N_{add.load} \\ M_{phase2} &= M_{add.load} \end{aligned} \tag{2}$$

where $N_{Phase2}, M_{Phase2}$ are the axial force and bending moment, respectively, in Load Phase 2,

$N_{design}$ is the axial force designated in the design, and

$N_{Add.load}, M_{Add.load}$ are the axial force and bending moment due to the additional load.

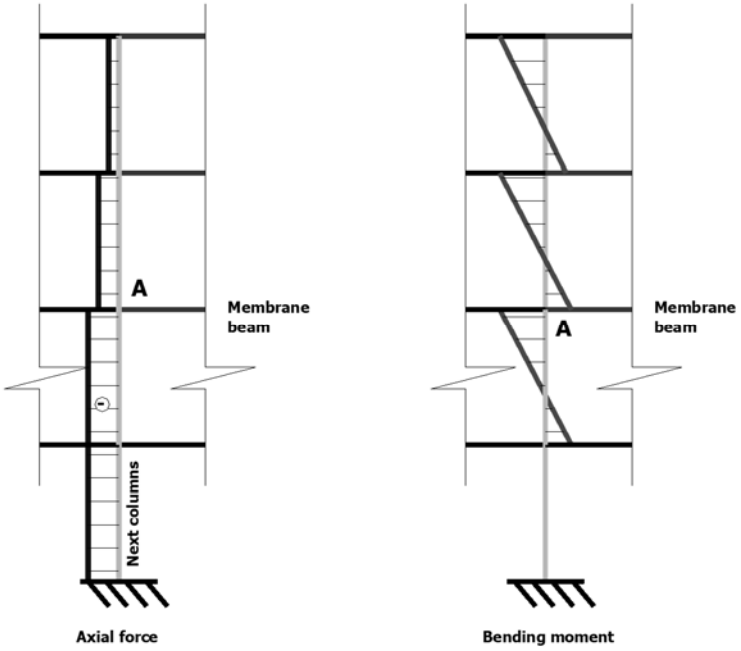


Fig. 13: Adjacent column's internal forces

### 5.5 Conclusion

The response of the residual frame has been once again explained but this time in an extended zone in order to highlight the behavior of the adjacent columns. Moreover, the so-called "arch" effect has also been demonstrated. Next, the results proved the influence of the column's deformation on the arch effect. The most dangerous positions were estimated by understanding of the behavior of two specific parts. Finally, some remarks were made in order to show the member behavior in detail, a subject which is treated further in the next section.

## 6 DEVELOPMENT OF THE SUBSTRUCTURE MODEL

This section concentrates on the development of the extended substructure of the zone in Fig. 1. The requirements of extraction were based on the results given in previous sections. Furthermore, the relation between the arch effect and column deformation will be analyzed in order to highlight the frame's role in triggering the development of the alternative load path.

Before moving on to details of this model's development, the two basic positions of the damaged column will be presented to highlight their differences. Fig. 14. repeats the diagram of the two alternative load paths corresponding to external and internal damage.

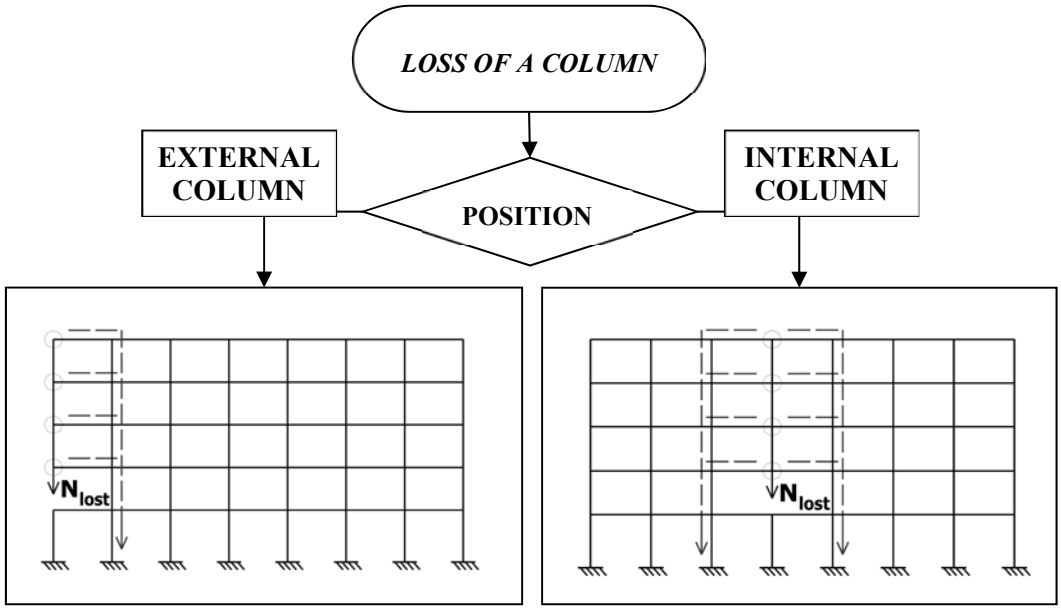

Fig. 14: Two alternative load paths

### 6.1 Requirements for extraction

Section 5 mainly presented the alternative load path of the residual frame resulting from internal damage. As was explained in that section, the arch effect appears due to the deformation of the adjacent columns when they compress the top beam. However, in the case of external damage, the end points on one side of the beam are free. Hence, no arch effect occurs.

Fig. 15 illustrates the full residual frame in which specific positions in the substructure are identified by colors. There are 3 requirements for ensuring an accurate damage model:

First requirement: Continuity

The adjacent column receives the bending moment transferred from the directly affected part as a function of the stiffness distribution. So, it is required that the adjacent columns, the equivalent beam and the beams on the adjacent span be connected as in a real frame. The full model has to cover the extended zone in Fig. 14.

Second requirement: Compatibility

It has been shown that the bending moment distribution at the point where the equivalent beam, adjacent column and adjacent span beam connect depends on their bending stiffness. For example, when the adjacent span beam receives the bending moment, it distributes the moment to the other end depending on the rotational capacity of its end points (the green zones numbered 1, 2, 3 and 5, 6, 7 in Fig. 15). Another transfer point is the position with the same influence but on the column, which is presented by the red zone at the adjacent column's end point (zones 4 and 8).

Third requirement: Horizontal restraint

The arch effect may be triggered within the frame. This is represented by the axial forces that appear in the equivalent beams due to the deformation of the adjacent columns. However, that movement of the column's end points is influenced by the horizontal stiffness of the frame. In Fig. 15, that part is defined by a blue rectangle on both sides (numbered 9 and 10).

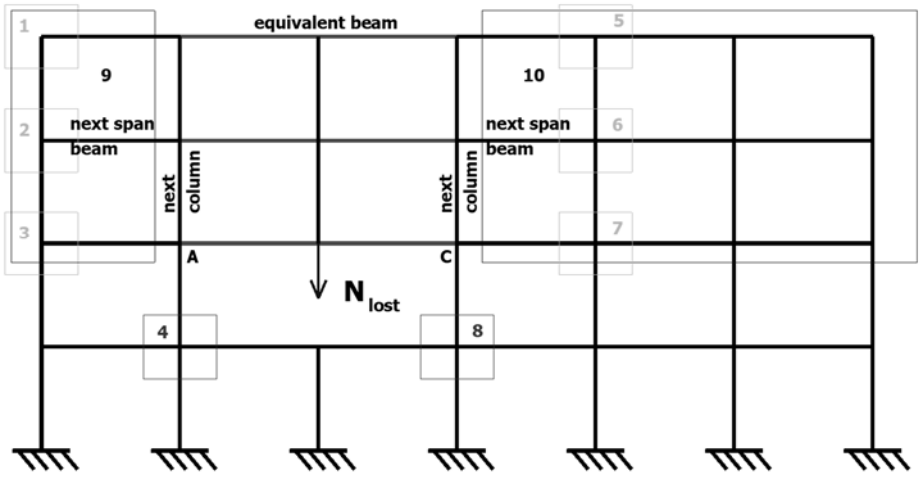


Fig. 15: Specific identified zones

## 6.2 Beam/column partial end restraints

In order to keep the rotational capacity of the adjacent span beam's end point as it is in the real residual frame, the rotational stiffness ***Ks*** was defined. It included the bending stiffness of all elements within the first and second levels expanding from the connection point. The calculation is presented here in Fig. 16.

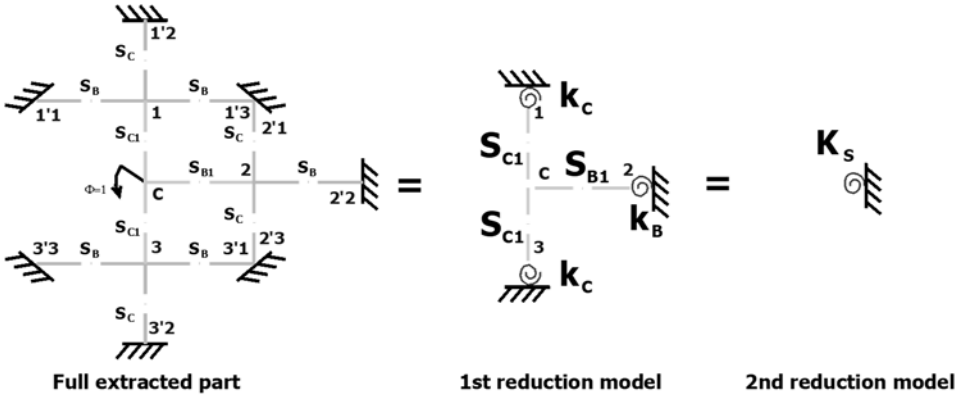


Fig. 16: The development of the formula for ***Ks***

## 6.3 Horizontal restraint

Fig. 17 illustrates the method for predicting the horizontal restraint coefficient. In fact, the movement of point 7 in Fig. 15, when supporting the axial force of the membrane beam, is limited by the stiffness of the members within the blue dashed rectangle. That stiffness is mainly bordered by two floors: the one below and the one above the loaded floor.

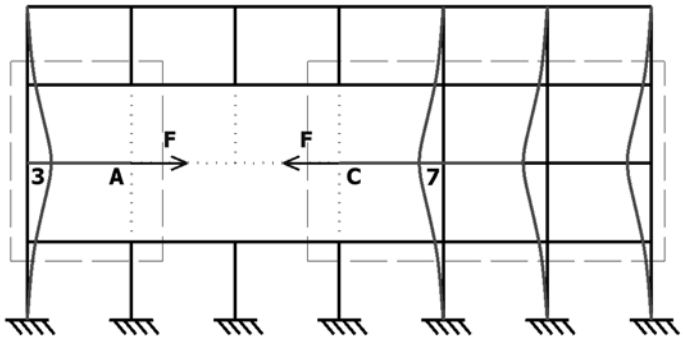

Fig. 17: Horizontal restraint definition

## 6.4 Unbraced part

This structural model with the perfect restraint system was presented first by Wong (2005), who used this analysis to calculate the resistance of a frame in a fire. In particular, in the model, the column supports a lateral force. As a result, it behaves like a beam instead of a column. So, as a beam, it undergoes a tensile force at the end and is elongated. In this way, it works as a tensile member. In Fig. 18, the model is extracted from the frame.

This thesis defines the partially restrained stiffness applied to the column end in order to simulate the continuity of the extracted model in relation to surrounding members.

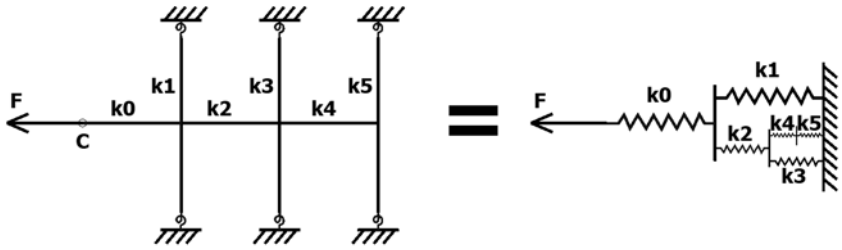

Fig. 18: The development of the model and its stiffness

The model's stiffness was taken from the relation between the connected members. For example, the column's stiffness $k_5$ connects to the beam's stiffness $k_4$ at the loaded point, then the stiffness at equilibrium $K_{eq(4,5)}$ was obtained by the serial connection rule. Next, the column's stiffness was connected to the group (4,5) at the end of beam 4, then $K_{eq(3,4,5)}$ was treated as the group (4,5) parallel connected to column $k_3$. Consequently, the horizontal restraint coefficient $K^{UnBraced}_{(3columns)}$ equals the total of group $(k_0, k_1, k_2, k_3, k_4, k_5)$.

$$\frac{1}{K^{UnBraced}_{(3columns)}} = \frac{1}{k_0} + \frac{1}{k_1 + \dfrac{1}{\dfrac{1}{k_2} + \dfrac{1}{k_3 + \dfrac{1}{\dfrac{1}{k_4} + \dfrac{1}{k_5}}}}} \tag{3}$$

where $K^{UnBraced}_{(3columns)}$ is the horizontal restrained coefficient of point C, and

$k_i$ is the beam or column stiffness.

## 6.5 Braced part

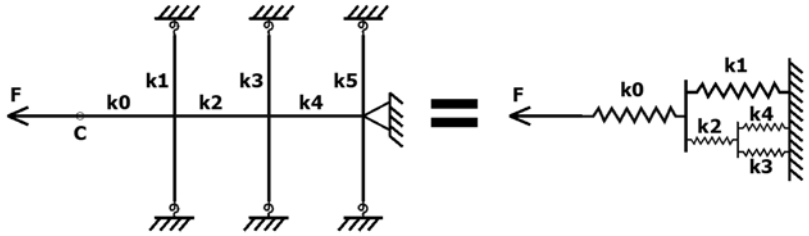


Fig. 19: The braced part

The development of this model was simpler than for the unbraced case. Given the assembly rule, the displacement of the right loaded point was calculated like the unbraced part, but with a small change in configuration. Namely, the end of the beam is braced, so the member $k_5$ is out of work. As a result the connection rule changes at the first connected member and the stiffness of the whole group mainly comes from the axial stiffness of the beam.

So, the displacement of the braced side's loaded point equals

$$\frac{1}{K^{Braced}_{(3columns)}} = \frac{1}{k_0} + \frac{1}{k_1 + \frac{1}{\frac{1}{k_2} + \frac{1}{k_3 + k_4}}} \tag{4}$$

Where $K^{Braced}_{(3columns)}$ is the horizontal restrained coefficient of point C in the braced frame.

## 6.6 Equivalent adjacent span beam

The previous horizontal restraint coefficient was applied to the extended model to define a new concept: *equivalent adjacent span beam*. This term replaces the original adjacent span beam by the beam with the same bending ability but a new lengthening capacity. For example, the equivalent beam on the right side at the level 3 (level of membrane beam) has the value

$$A_{equ3.right} = \frac{K^{Un-braced}_{(3columns)} L_B}{E_B} \tag{5}$$

where $A_{equ3.right}$ is the equivalent adjacent span beam's cross section area on the right,

$L_B$ is the adjacent span beam length, and

$E_B$ is the elastic modulus of the beam.

## 6.7 Extended substructure

Fig. 20 demonstrates the substructure which resulted from the extraction process. The full residual frame with colored borders is presented in Fig. 20.a. On the right side, the extracted substructure uses the same colors in order to represent the model and its included members.

This model takes the directly affected part, in magenta, as the core cause of the deformation of the adjacent columns. The additional load $N_{lost}$ is placed at the midpoint of the membrane beam AC. The adjacent columns zones, targeted in the study of this substructure, are connected to the end of the equivalent beam. Due to the distribution of internal forces within the column, the adjacent columns zone is limited to points 4 and 8. The columns below the damaged column are neglected in this model. To maintain the continuity of this column section with respect to the lower part, the column's bottom end point is defined by the partially restrained coefficient.

As defined earlier, the arch effect represents the phenomenon of axial forces appearing in the equivalent beam due to the deformation of the adjacent columns. Those deformations are influenced by the distribution of bending stiffness of the members connected to the column's end. So, the adjacent span beams are also included in this model with the necessary modifications, i.e., in the equivalent adjacent span beam.

The first modification involves the partially restrained beam end's conditions. Once again, the beam end's condition maintains the continuity of the model with respect to the whole frame. It is calculated as the bending capacity of the beam's end point according to the bending stiffness of the connected members.

The last but most important modification applied to the adjacent span beam is the equivalent lengthening stiffness. That concept is represented analytically by the horizontal movement capacity of the column's end points. It includes the capacity of one floor on one side of a beam axial stiffness.

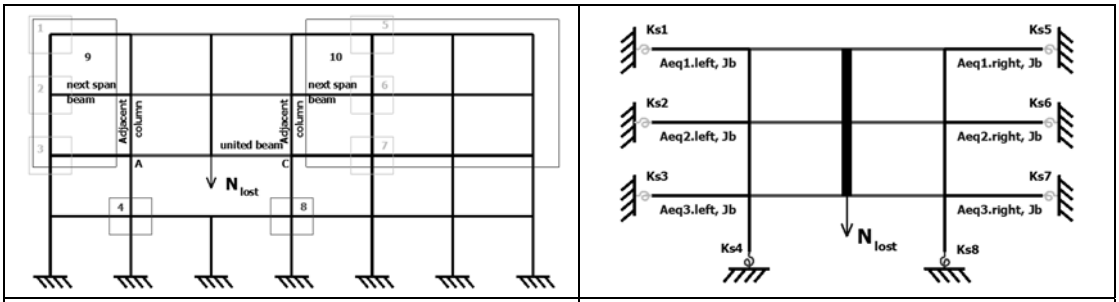


(a) Original residual frame | (b) Substructure

Fig. 20: The original residual frame and the full model (internal damage)

The same process is applied to extract the model from the frame in the case of an external damaged column. Fig. 21 illustrates the same process as in Fig. 20 for external damage.

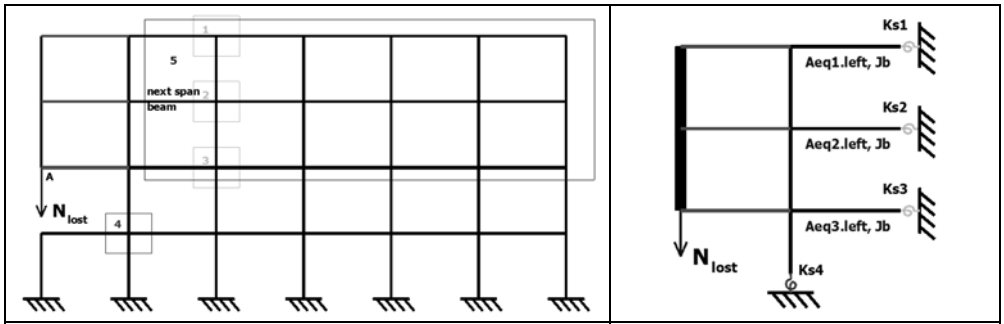


(a) Original residual frame | (b) Substructure

Fig. 21: The original residual frame and the full model (external damage)

## 6.8 Conclusion

This section finished the analytical model in order to estimate the behavior of the second part in the alternative load path – the adjacent column zone. This investigation also presents two critical positions in the alternative load path: the top equivalent beam supporting compression and the adjacent column supporting the pair (M,N). They are the dangerous points which could cause the collapse of the frame even if the directly affected part manages to support the additional load.

Three parameters were calculated to ensure an accurate portrayal of the full substructure. The first parameter was the partial restraint coefficients. As in Section 6, in one frame, there are only 4 values of $K_S$. The column end's restraint coefficient was calculated using the same method. The last parameter was the equivalent cross section of the adjacent span beam. For each floor, it is necessary to estimate at least one value.

With the requirements demonstrated in Section 6.1, the substructure's parameters were defined as intricately as was necessary. So, more simplification was needed for practical purposes.

# 7 ADJACENT COLUMN'S KEY ELEMENT AND RESISTANCE

The content of this section concentrates on the key elements of the alternative load path. Those elements are the critical elements which are present in certain dangerous conditions due to the loss of a column. Using the definition of *progressive collapse*, the frame collapse is identified when a second member is damaged.

This section points out the most dangerous positions in the investigated zone of the frame. Their critical resistances are discussed in order to apply the robustness assessment afterwards. Fig. 22 presents the behavioral load-carrying curve with a remark on possibilities for instability.

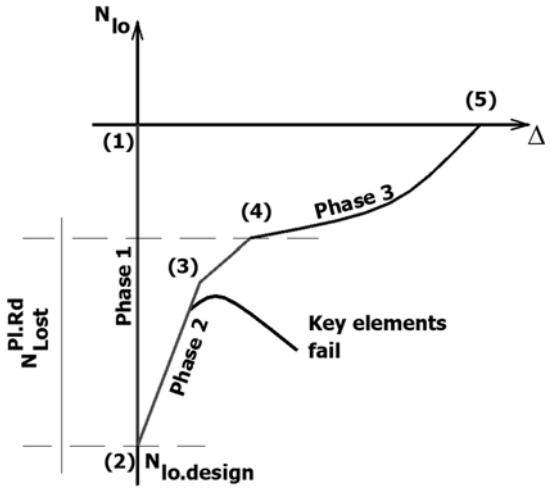


Fig. 22: Moment where frame could collapse due to the loss of second key element

## 7.1 Key elements and the loading status

In the extended substructure, the most dangerous positions are the equivalent beam end section in pair (***M, +N/-N***), the adjacent column in (***M, N***) and the middle beam under tension. If one of these members fails, the frame will collapse before point (2). The internal force magnitudes were estimated for the specific point on the load-carrying curve in Fig. 23.

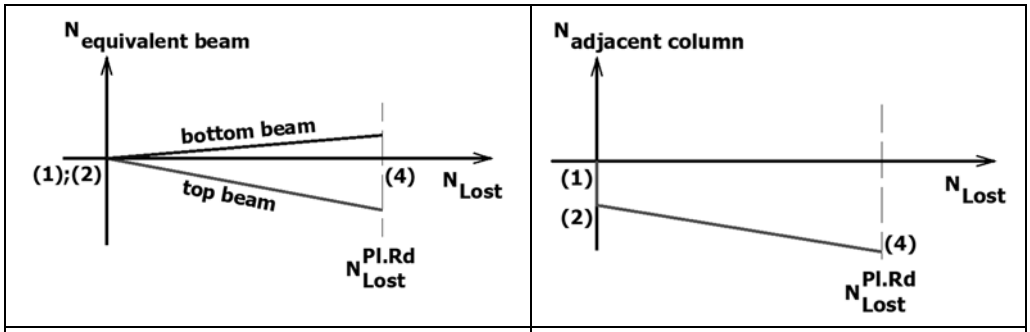


(a) Equivalent beam axial forces | (b) Adjacent column axial force

Fig. 23: Axial forces in the key elements

Fig. 24 repeats the substructure in which the key members are illustrated. Those key members' survival will ultimately determine the frame's robustness in Load Phase 2.

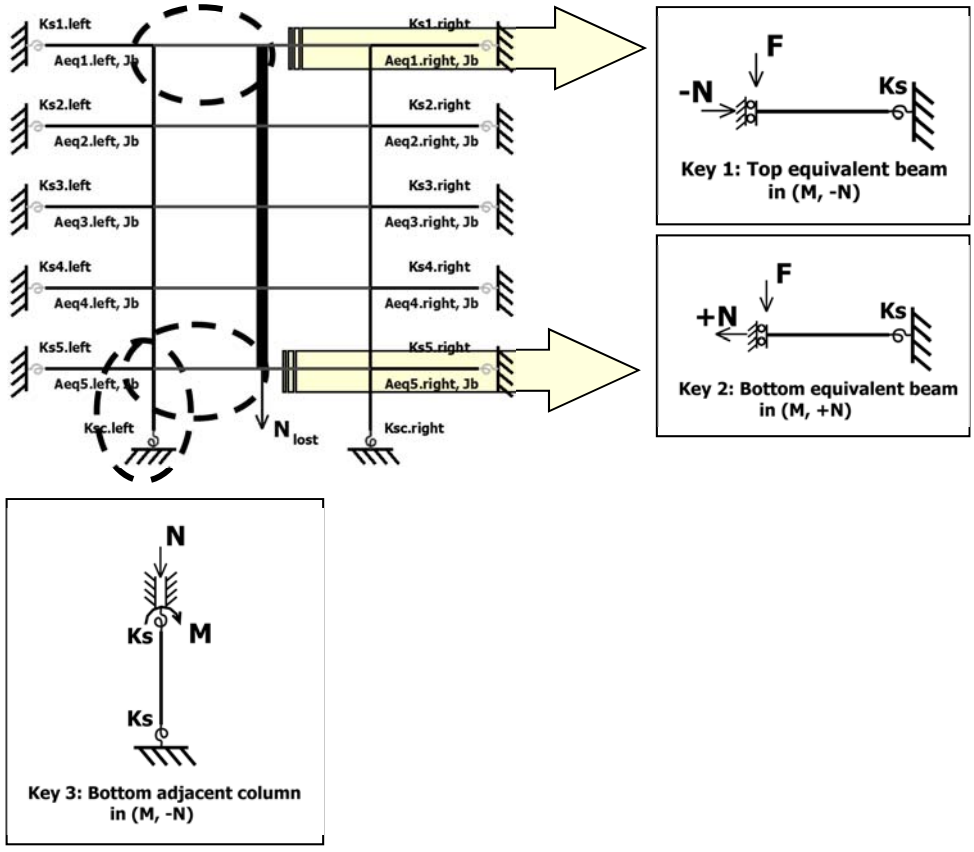


Fig. 24: General model and the key elements

## 7.2 Element stability check

From the results, two dangerous positions have been identified: the equivalent beam in compression and bending simultaneously, and the adjacent column in compression and bending.

With the special load-carrying curve applied to these key elements, each element must be checked not only for plastic resistance but also for stability. The next paragraph demonstrates the stability test for the bottom adjacent column. In the typical frame, it is the most dangerous member.

In the Phase 2, the top point of the column does not move. The bending moment and the axial force increase in the adjacent column. Due to $N_{lost}$, the compression force increases linearly in the adjacent column, as does the bending moment. The $N$ and $M$ applied to the column are the result of the vertical load $N_{lost}$. They are a linear function of $N_{lost}$. In other words, $N$ is the linear function of $M$ and vice versa. With that $M$, $N$ pair, the check is done by the following formula. The formula is derived from EUROCODE 3, for column stability estimation.

$$\Rightarrow 0 \le \frac{N_{Sd}}{N_{pl.Rd}} \le \frac{A_w}{A}$$

$$M_{N.y.Rd} = M_{pl.y.Rd}\left[1-\left(\frac{N_{Sd}}{N_{pl.Rd}}\right)^2 \frac{1}{2\left(\frac{h-t_f}{h-2t_f}\right)\left(1-\frac{A_w}{A}\right)\frac{A_w}{A}+\left(\frac{A_w}{A}\right)^2}\right] \tag{6}$$

$$\Rightarrow \frac{A_w}{A} \le \frac{N_{Sd}}{N_{pl.Rd}} \le 1$$

$$M_{N.y.Rd} = bt_f\left(h-t_f\right)f_y - \frac{1}{2}\left(N_{Sd}-A_w f_y\right)\left[\left(h-2t_f\right)+\frac{N_{Sd}-A_w f_y}{2bf_y}\right]. \tag{7}$$

where

| | | |
|---|---|---|
| | $N_{Sd}$ | is the axial force apply on the column |
| | $N_{Pl.Rd}$ | is I section's axial resistance. |
| | $M_{Pl.Rd}$ | is I section's pure bending moment resistance. |
| | $M_{N.y.Rd}$ | is I section's bending moment resistance interact with applied $N_{Sd}$. |
| | $A$ | is area of I section. |
| | $A_w$ | is web area of I section. |
| | $t_f$ | is I section's flange thickness. |
| | $h$ | is height of I section. |

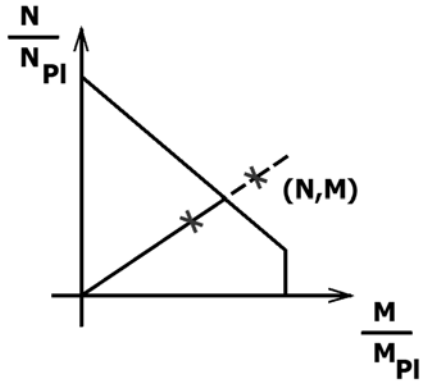


Fig. 25: Frame member section stability check

### 7.3 Conclusion

The extended substructure was developed to calculate the distribution of internal forces in the whole frame. On a specific point of the load-carrying curve in Fig. 2, the internal forces of each member on the load path were predicted. Based on that knowledge of the individual members' loading status, the design check procedure was carried out.

## 8 VALIDATION PROCEDURE AND NUMERICAL TOOLS

This section introduces the validation approaches for later analytical simulations and the numerical tools used. Also, Level 1 and Level 2 are described in systematic detail, namely regarding the validation procedures which correspond to the simulation steps.

### 8.1 Multilevel validation method

The full 2-level extraction procedure, which is demonstrated in Fig. 26, is repeated below to illustrate the creation of the substructure model and its validation approaches.

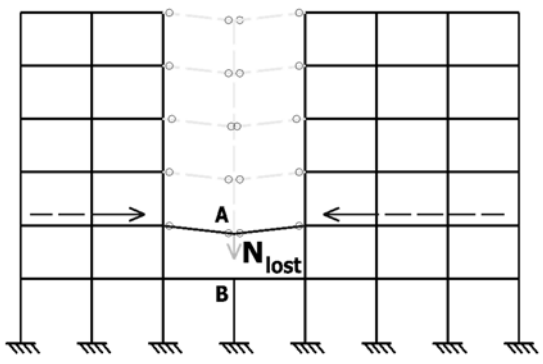


| Level 1 | Level 2 |
|---|---|
| Frame investigation | Substructure analytical model |

Fig. 26: The 2-levels extraction

In the *frame level*, according to the loading process defined section 2, the frame was first simulated using numerical tools. The tools used are two finite element programs: OSSA2D and FINELG. Then, full-scale linear and nonlinear investigations were carried out on the frame supporting normal and abnormal loads. Next, parametrical investigations were performed which focused on the distribution of internal forces within the frame throughout the accidental event. Finally, the load transfer flow was drawn out, which defined the alternative load path developed in such an abnormal situation. Thus, the structural members which influence the frame's behavior were identified.

In the substructure level, the extracted substructure was simulated by a simplified analytical model. Firstly, from the parametrical investigation, the influences of the surrounding structure on the isolated member were recorded. They have been defined by the boundary conditions of the individual member and by the specific load applied to it.

Next, in the second step, the analytical behavior of the individual member was simulated and simplified in order to create a more manageable analytical formula.

In the last step, the individual members were assembled according to conditions of continuity. These conditions were also simplified, forming the practical model.

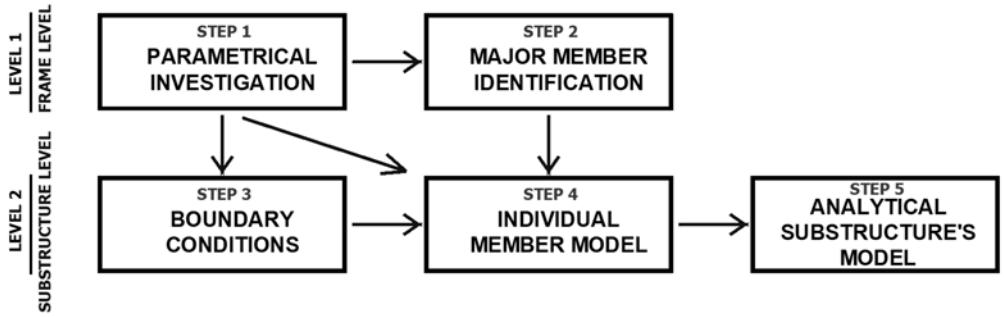


Fig. 27: The procedures for building the analytical substructure model

Then, three separate validations were performed:

- The validation of the single member boundary condition.
- The validation of the single model simulation.
- Last, but most importantly, the validation of the simplified zone model.

The validation process has been applied to each step of the analytical simulation according to the procedure demonstrated above. So, the next section provides a short description of two numerical tools which were used in the validation process.

## 8.2 Numerical tools

The first software used for this purpose was FINELG, a non-linear finite element program that has been developed for decades at the $MS^2F$ Department, ArGEnCo, University of Liege. The computer program FINELG is a finite element program used to solve

- geometrically and materially nonlinear solid or structural problems under static dead loads;
- linear and nonlinear instability problems, leading to buckling loads and instability modes by an eigenvalue computation;
- dynamic problems, leading to Eigen frequencies and vibration modes taking account, or not, of the internal stresses.

The 2-node classic plane beam element number 33 was used to model the 2-D frames investigated. Each node has 3 degrees of freedom ($\boldsymbol{u}$, $\boldsymbol{v}$ and $\boldsymbol{\theta}$ - see Fig. 28). Plasticity and residual stress could be considered for any cross section. However, residual stress was not included in this

work in light of the author's aim of understanding the global behavior of the frame, not local problems. Non-linear bending springs could be applied to the node along the $\theta$ direction.

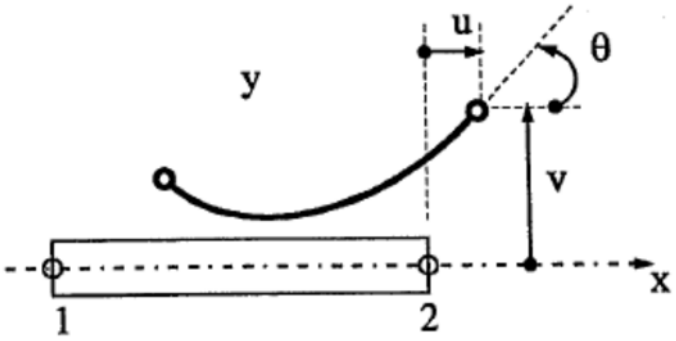


Fig. 28: Classic beam element used in FINELG and OSSA2D [Finelg manual]

With this type of element, a linear law (Hooke's law) is used for elastic analyses and a bilinear elasto-perfectly plastic for non-linear analyses.

For simpler numerical simulations, such as single member validation or frame response in elastic ranges, the other FEM software, OSSA2D, is used.

OSSA2D is a program for linear elastic analysis using the method of displacements applied to plane structures formed by beams and bars. Those members are connected by rigid, hinge or semi-rigid connections, and many types of loads can be applied to the structure. The program's objective is to predict a frame's mechanical behavior quickly to engineers.

Unlike the FINELG program described above, OSSA2D's limits in elastic and geometric second-order analyses of plane frames are well suited to our purposes. The main element used in OSSA2D is the 2D classic beam element.

### 8.3 Validation

The validity of the analytical procedures proposed was verified by comparisons with the numerical results. An example of one of the frames analyzed is presented here below.

The frame has 7 spans and 6 floors, where the span length and the floor height are uniform. The column sections are HE360A and the beam sections are IPE400v. For this building, twelve positions of the lost column were investigated as presented in Fig. 29.

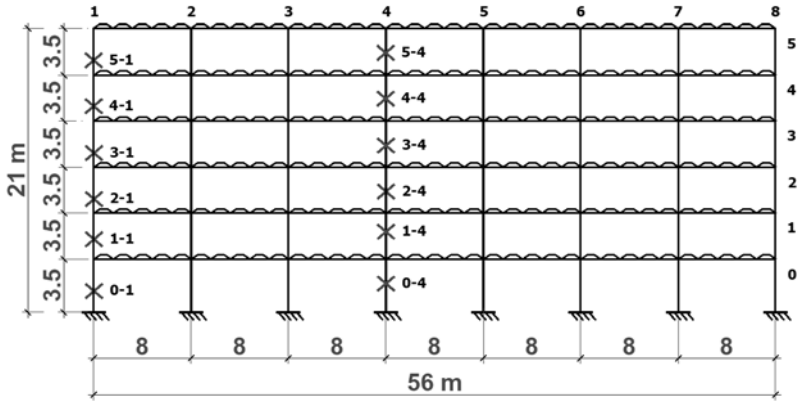


Fig. 29: Frame investigated.

Fig. 30 demonstrates the first validation step, where a single, 6-meter high HE180A column supported a compressed load of 510 kN. The two end points of the column were connected to springs of 15,000 and 25,000 kNm/rad. The analytical results of the first- and second-order stiffness are included here with a comparison to data from FINELG.

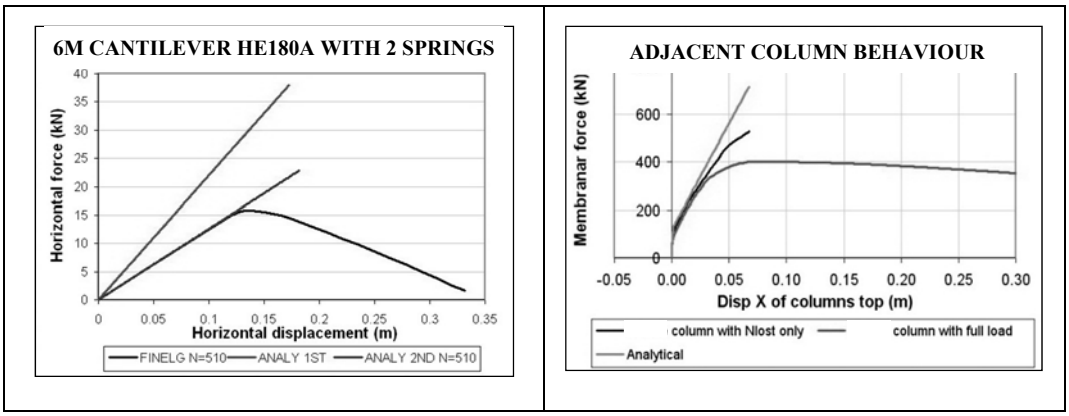


Fig. 30: Single analytical model validation

Next, the frame in Fig. 29 with full loads being applied was investigated. Fig. 31 shows the column extracted next to position 1-4 and its analytical results. The partial restraint coefficients were taken out of the frame configuration and applied to the simulated model. In it, the analytical prediction obtained through the proposed procedures has been compared to the response obtained through a fully non-linear numerical analysis.

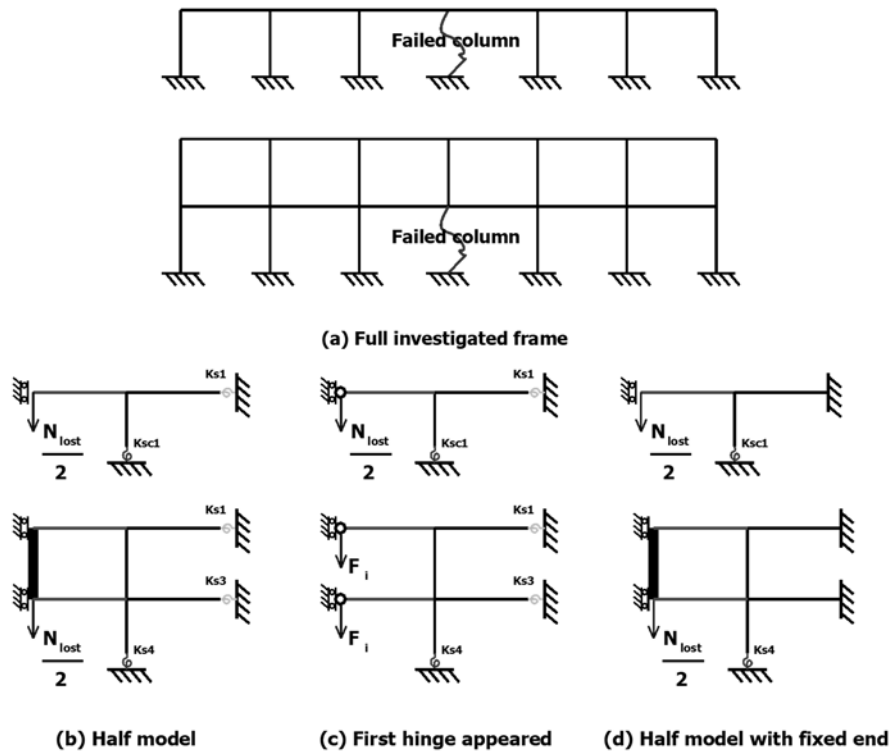


Fig. 31: The first and second frames and models for validation

Table 7.1. The error percentages of the 20-storey frame (resistance in kN)

Elastic

Frame: 4 storey x 11 spans  Position: 0-4  IPE400V

| Section | Top beam | | | | | Bottom beam | | | | |
|---|---|---|---|---|---|---|---|---|---|---|
| | OSSAD | Model | Fixed mod | % model | % fixed | OSSAD | Model | Fixed mod | % model | % fixed |
| HE 100A | -8.91 | -10.270 | -9.620 | -15.26 | -7.97 | 4.44 | 5.170 | 4.830 | -16.44 | -8.78 |
| HE 160A | -33.34 | -39.200 | -36.910 | -17.58 | -10.71 | 15.92 | 18.680 | 17.600 | -17.34 | -10.55 |
| HE 200A | -58.09 | -67.750 | -64.670 | -16.63 | -11.33 | 26.26 | 30.280 | 29.030 | -15.31 | -10.55 |
| HE 240A | -87.85 | -100.420 | -97.400 | -14.31 | -10.87 | 36.31 | 40.670 | 39.710 | -12.01 | -9.36 |
| HE 300A | -123.37 | -136.410 | -134.370 | -10.57 | -8.92 | 43.62 | 46.710 | 46.300 | -7.08 | -6.14 |
| HE 340A | -138.46 | -150.460 | -148.990 | -8.67 | -7.61 | 44.58 | 46.500 | 45.640 | -4.31 | -2.38 |
| HE 360A | -144.17 | -155.490 | -154.250 | -7.85 | -6.99 | 44.46 | 45.810 | 45.640 | -3.04 | -2.65 |
| HE 400A | -152.86 | -162.660 | -161.770 | -6.41 | -5.83 | 43.58 | 43.860 | 43.770 | -0.64 | -0.44 |
| HE 450A | -160.61 | -168.190 | -167.610 | -4.72 | -4.36 | 41.7 | 40.760 | 40.720 | 2.25 | 2.35 |
| HE 500A | -165.72 | -170.790 | -170.420 | -3.06 | -2.84 | 39.36 | 37.410 | 37.390 | 4.95 | 5.01 |

1st hinge

Frame: 4 storey x 11 spans  Position: 0-4  IPE400V

| Section | Top beam | | | | | Bottom beam | | | | |
|---|---|---|---|---|---|---|---|---|---|---|
| | OSSAD | Model | Fixed mod | % model | % fixed | OSSAD | Model | Fixed mod | % model | % fixed |
| HE 100A | -22.280 | -25.960 | -23.570 | -16.52 | -5.79 | 10.840 | 12.780 | 11.560 | -17.90 | -6.64 |
| HE 160A | -79.720 | -94.770 | -87.430 | -18.88 | -9.67 | 37.300 | 44.290 | 40.960 | -18.74 | -9.81 |
| HE 200A | -133.430 | -157.250 | -148.230 | -17.85 | -11.09 | 59.040 | 68.830 | 65.290 | -16.58 | -10.59 |
| HE 240A | -193.740 | -223.590 | -215.410 | -15.41 | -11.19 | 78.300 | 88.500 | 85.990 | -13.03 | -9.82 |
| HE 300A | -261.450 | -291.540 | -286.380 | -11.51 | -9.54 | 90.570 | 97.600 | 96.580 | -7.76 | -6.64 |
| HE 340A | -289.120 | -316.660 | -313.040 | -9.53 | -8.27 | 91.410 | 95.830 | 95.280 | -4.84 | -4.23 |
| HE 360A | -299.430 | -325.400 | -322.360 | -8.67 | -7.66 | 90.780 | 93.960 | 93.550 | -3.50 | -3.05 |
| HE 400A | -314.900 | -337.490 | -335.330 | -7.17 | -6.49 | 88.450 | 89.350 | 89.120 | -1.02 | -0.76 |
| HE 450A | -328.410 | -316.190 | -344.790 | 3.72 | -4.99 | 84.200 | 82.540 | 82.430 | 1.97 | 2.10 |
| HE 500A | -337.060 | -349.510 | -348.600 | -3.69 | -3.42 | 79.200 | 75.420 | 75.370 | 4.77 | 4.84 |

Moreover, the validations performed on the typical frame substructures have been organized into 5 frame types. Fig. 31 presents the first and second frame types used for the validations. The first frame type was 6 spans x 1 floor. The beam length was 8m and column height was 3.5m. The beam sections were IPE400V. The columns sections ranged from 10 sections: HE 100A, 160A, 200A, 240A, 300A, 340A, 360A, 400A, 450A and 500A. The beam length and column height remained constant.

Three types of half models were carried out. They were the half model with the equivalent adjacent span beam, the half model with fixed beam ends and the model simulating the situation when the first hinge appears at the midsection. Fig. 31.b, c, and d demonstrate these models. There is a model for the first hinge situation but with fixed beam ends.

The other types of frames were modeled like the two previous frames. However, the third, fourth and fifth frames were 11 spans x 4 floors, 11 spans x 15 floors and 4 spans x 20 floors, respectively.

In Table 7.1, the errors decreased following the increase in the number of column sections. However, with the applied load's magnitude being 500 kN, which represented a 1000 kN additional load, the error in the value of the top beam's compression is not so significant.

# 9 MAIN ACHIEVEMENTS RELATED TO THE GLOBAL BEHAVIOR OF THE FRAME FOLLOWING THE LOSS OF A COLUMN

## 9.1 Prediction of the two alternative load paths activated within the frame

When a column is damaged within the frame, the frame goes from its initial state to a residual state. Due to the change in the frame's physical character, the forces flowing within the frame must change their path to reach the foundation. Thus, these paths appear in the frame because of the additional load. Influenced by the particular properties of different structures, the alternative load path is activated within the frame, a phenomenon represented by the redistribution of internal forces. The results obtained from the author's numerical investigations on the frames in such an accidental

event proved the presence of these alternative load paths. Each alternative load path has been defined herein in order to identify the chain of structural members which must support the additional load.

### 9.1 Investigation on the redistribution of the internal forces within the frame after the accidental event through the simplified analytical model

In the process of investigating the alternative load path, the distribution of internal forces was obtained. Through the simulation of the directly affected part in the real frame by the simplified analytical model, the fundamental behavior of the part was illustrated. The results obtained were then compared to the FEM analysis. In the end, the validation proved the substructure's ability to accurately represent the real frame's behavior at the specific point selected at the top of the damaged column.

A new model was extended from the previous analytical model in order to calculate how the forces act on each member within the alternative load path. Their loading states were used to measure the frame's ability to maintain the alternative load path after the accidental event. In turn, this ability determined the robustness of the frame. Also, the special distribution of the internal forces within the frame, called the "arch effect", was identified and estimated.

**LITERATURE**


[1] DEMONCEAU J.F., LUU H.N.N. & JASPART J.-P., *Recent investigations on the behaviour of buildings after the loss of a column*, Proceedings of the International Conference in Metal Structures, Poiana Brasov, Romania, 2006.

[2] DEMONCEAU J.-F., Steel and composite building frames: sway response under conventional loading and development of membranar effects in beams further to an exceptional action, PhD thesis presented at Liège University, 2008.

[3] DEMONCEAU, J.F.; JASPART, J.P.,. *Experimental test simulating the loss of a column in a composite building – Liège University*. Internal report for the RFCS project RFSCR-04046 "Robust structures by joint ductility", Liège University, September 2006.

[4] DEMONCEAU,J.-F.; LUU, H.N.N.; JASPART, J.-P., Development of membranar effects in frame beams: Experimental and analytical investigations, Eurosteel conference in Gratz, 2008.

[5] ELLINGWOOD, B. R.; SMILOWITZ, R.; DUSENBERRY, D. O.; DUTHINH, D.; LEW, H.S.; CARINO, N. J, *Best Practices for Reducing the Potential for Progressive Collapse in Buildings*, National Institute of Standards and Technology, Technology Administration, U.S. Department of Commerce, February 2007.

[6] ELLINGWOOD, B.; LEYENDECKER, V, *Approaches for Design Against Progressive Collapse*, Journal of the Structural Division, March1978, pp. 413-423(11).

[7] FINELG user's manual. Non-linear finite element analysis software. Version 8.2, July 1999.

[8] IZZUDDIN, B.A.; VLASSIS, A.G. ELGHAZOULI, A.Y. & NETHERCOT, D.A., *Progressive collapse of multi-storey buildings due to sudden column loss – Part I: Simplified assessment framework*. Engineering Structures, 2007 (doi:10.1016/j.engstruct.2007.07.011).

[9] IZZUDDIN, B.A.; VLASSIS, A.G. ELGHAZOULI, A.Y. & NETHERCOT, D.A., *Progressive collapse of multi-storey buildings due to sudden column loss – Part II: Application.* Engineering Structures, 2007 (doi:10.1016/j.engstruct.2007.08.011).

[10] IZZUDDIN, B.A.; VLASSIS, A.G. ELGHAZOULI, A.Y. & NETHERCOT, D.A., *Assessment of progressive collapse in multi-storey buildings*. Proceedings of the Institution of Civil Engineers – Structures & Buildings 160 – Issue SBI, 2007.

[11] KHANDELWAL, K.; TAWIL, S, *Progressive Collapse of Moment Resisting Steel Frame Buildings*, Proc. of the 2005 Structures Congress and Forensic Engineering symposium, New York, April, 2005.

[12] KRAUTHAMMER, T.; HALL, R. L.; WOODSON, S. C.; BAYLOT, J. T.; HAYES, J. R, *Development of Progressive Collapse Analysis Procedure and Condition Assessment for Structures*, Proc. of Workshop on Prevention of Progressive Collapse Multihazard Mitigation, Council of National Institute of Building Sciences, U.S.A, 10-12 July, 2002.

[13] MULLERS, I.; VOGEL, T, *Robustness of Reinforced Concrete Structures Subjected to Column Failure*, Proceedings of the 2nd FIB Congress, FIB Italy, , Vol. 2, Naples, 2006, pp. 592-593.

[14] SMILOWITZ, R, *Analytical tools for Progressive Collapse Analysis*, Proc. of Workshop on Prevention of Progressive Collapse Multihazard Mitigation, Council of National Institute of Building Sciences, U.S.A, 10-12 July, 2002.

[15] STAROSSEK, U, *Progressive collapse of structures-Invited Lecture*, The 2006 Annual Conference of the Structural Engineering Committee of the Korean Society of Civil Engineers, Seoul, Korea, May 25, 2006.

[16] STAROSSEK, U, *Typology of progressive collapse*-Engineering Structures 29 (2007) 2302–2307.

[17] STAROSSEK, U.; *Progressive Collapse of Bridges, Aspects of Analysis and Design*, International Symposium on Sea-Crossing Long-Span Bridges, Mokpo, Korea, Feb. 15-17, 2006.

[18] WONG, M.B, Modelling of axial restraints for limiting temperature calculation of steel members in fire, Journal of Constructional Steel Research 61 (2005) 675–687.

**Reviewers:**

Ing. Kološ Ivan, Ph.D., Department of Structural Mechanics, Faculty of Civil Engineering, VŠB – Technical University of Ostrava, Czech Republic.

Prof. Ing. Norbert Jendželovský, PhD., Department of Structural Mechanics, Faculty of Civil Engineering, Slovak University of Technology in Bratislava, Slovakia.